

Pearl-Necklace-Like Local Ordering Drives Polypeptide Collapse

Suman Majumder,¹ Ulrich H. E. Hansmann,² and Wolfhard Janke¹

¹*Institut für Theoretische Physik, Universität Leipzig, Postfach 100 920, 04009 Leipzig, Germany*

²*Department of Chemistry and Biochemistry, University of Oklahoma, Norman, Oklahoma 73019, USA*

(Dated: January 11, 2019)

Collapse of the polypeptide backbone is an integral part of protein folding. Using polyglycine as a probe, we explore the nonequilibrium pathways of protein collapse in water. We find that the collapse depends on the competition between hydration effects and intra-peptide interactions. Once intra-peptide van der Waal interactions dominate, the chain collapses along a nonequilibrium pathway characterized by formation of pearl-necklace-like local clusters as intermediates that eventually coagulate into a single globule. By describing this coarsening through the contact probability as a function of distance along the chain, we extract a time-dependent length scale that grows in linear fashion. The collapse dynamics is characterized by a dynamical critical exponent $z = 0.5$ that is much smaller than the values of $z = 1 - 2$ reported for non-biological polymers. This difference in the exponents is explained by the instantaneous formation of intra-chain hydrogen bonds and local ordering that may be correlated with the observed fast folding times in proteins.

Changing the solvent condition from good to poor renders an extended polymer to undergo a collapse transition by forming a compact globule [1, 2]. Both experiments [3, 4] and simulations [5, 6] indicate that a protein also experiences such a collapse transition while folding into its native state. However, the nonequilibrium dynamics of the collapse of proteins is only poorly understood and an active research topic [7]. Most previous studies consider only the hydrophobicity of apolar side chains of amino acids in a protein as driving force for collapse [8, 9]. In the present paper we focus instead on the contributions by intra-peptide interactions, present even for residues with no hydrophobic or only weakly hydrophobic side chains [10–13] where the collapse-driving forces are not necessarily proportional to the exposed surface. Our test system is polyglycine, and has been chosen to connect our work with recent studies of homopolymer collapse dynamics [14–17] that found nonequilibrium scaling laws as known for generic coarsening phenomena [18]. Our hope is to establish such scaling laws also for the collapse of proteins. As a first stride towards this goal, here, we explore the kinetics of collapse of polyglycine.

Collapse of homopolymers was first described by de Gennes’ seminal “sausage” model [19], but today the phenomenological “pearl-necklace” picture by Halperin and Goldbart [20] is more commonly used, both for flexible [14, 16, 17, 21–25] and semiflexible polymer models [26, 27]. In this picture the collapse begins with nucleation of small local clusters (of monomers) leading to formation of an interconnected chain of (pseudo-)stable clusters, i.e., the “pearl-necklace” intermediate. These clusters grow by eating up the un-clustered monomers from the chain and subsequently coalesce, leading eventually to a single cluster. Finally, monomers within this final cluster rearrange to form a compact globule.

Of central interest in this context is the scaling of the collapse time τ_c with the degree of polymerization N (the number of monomers). While scaling of the form $\tau_c \sim N^z$, where z is the dynamic exponent, has been firmly established, there is no consensus on the value of z . Molecular dynamics (MD) simulations provide much smaller values ($z \approx 1$) than Monte Carlo (MC) simulations ($z \approx 2$). This difference is often explained with the presence of hydrodynamics in the MD simulations, but a value $z \approx 1$ has been reported recently also for MC simulations [16]. The “pearl-necklace” stage or the cluster-growth kinetics can be understood by monitoring the time (t) dependence of the mean cluster size $C_s(t)$, the relevant length scale. By drawing analogy with coarsening ferromagnets, it has been shown that scaling of the form $C_s(t) \sim t^{\alpha_c}$ with growth exponent $\alpha_c \approx 1$ holds for flexible homopolymers [14, 16].

Protein collapse is much less understood. While it has been shown by modeling a protein as semiflexible heteropolymer that the equilibrium scaling of the radius of gyration R_g with N is random-coil-like in a good solvent and globule-like in a poor solvent [28, 29], there have been few attempts to explore nonequilibrium collapse pathways

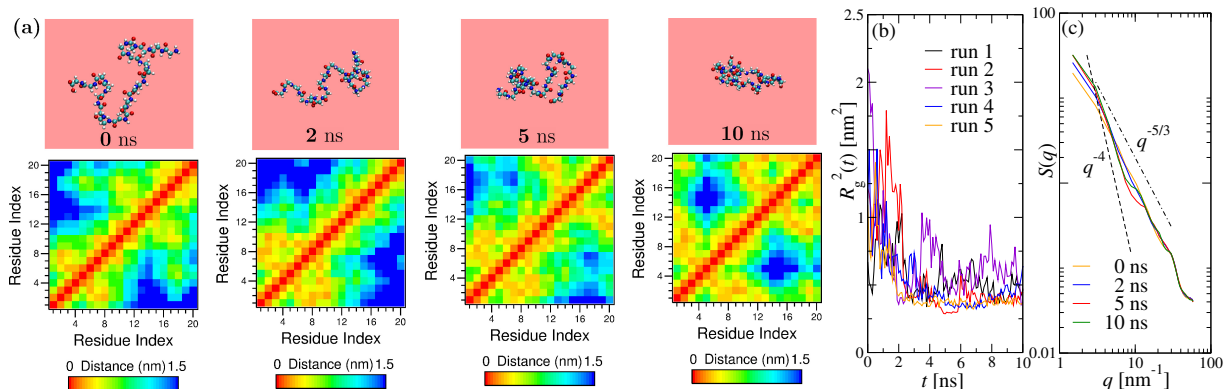


FIG. 1. **Time evolution of a short polypeptide.** a) The upper panel shows snapshots from the time evolution for collapse of $(\text{Gly})_{20}$ chain in water at $T_q = 290$ K, starting from an extended state at $t = 0$ ns. The lower panel shows the corresponding residue contact maps where two residues along the chain are in contact if the distance between them is less than 1.5 nm. (b) Time dependence of the squared radius of gyration $R_g^2(t)$ from five different runs. (c) Illustration of the structural evolution of the chain during the collapse shown via structure factor $S(q)$ as function of the wave vector q at the times presented in (a). The dashed lines with power-law decay exponent $5/3$ and 4 correspond to the expected behavior for an extended chain and crumpled globule, respectively.

[30, 31], and the corresponding scaling laws are not known. In order to probe the existence of such nonequilibrium scaling laws in protein collapse, we have simulated polyglycine chains $(\text{Gly})_N$ of various numbers N of residues. This choice allows us to probe in a systematic way the collapse of polypeptide chain, considering only homopolymers built from the simplest amino acid, glycine. Our results show that in water there is a *tug of war* between collapse-disfavoring hydration effects and collapse-favoring intra-peptide interactions. For longer chains ($N \geq 15$) the intra-peptide interactions win over the hydration effect leading to a collapse, making water in practice a poor solvent. We use these longer polyglycine chains to shed light on the collapse kinetics, with an emphasis on the presence of nonequilibrium scaling laws. Our results from all-atom MD simulations in the NVT ensemble using a hydrodynamics preserving thermostat (see the Method section for details), suggest a collapse mechanism that relies on fast local ordering by formation of pearl-necklace structures which eventually merge into a single globule. This process is characterized by a dynamic critical exponent $z = 0.5$ much smaller than the exponents $z = 1 - 2$ observed for non-biological polymers, and we speculate that this quicker local ordering and collapse enables the fast folding times seen in proteins.

We begin our analysis with a rather short chain, i.e., $(\text{Gly})_{20}$. The time evolution snapshots during the collapse in water at a temperature $T_q = 290$ K, well below the corresponding collapse transition temperature, are shown in Fig. 1(a). In a protein, collapse leads eventually to folding characterized by formation of distinct native contacts among the

residues. We show for this reason in the lower panel the residue contact maps where we define two residues as being in contact if they are within a distance of $r_c = 1.5$ nm. The red stripe along the diagonals depicts the self-contacts. The size of the extended (Gly)₂₀ chain is ≈ 2.0 nm, thus almost all the mutual distances between the residues fall under r_c . This makes it difficult to capture segregation or formation of any local structures on length scales comparable to r_c . Only late in the trajectories do we find a signature for loop formation, which is also apparent in the snapshot at $t = 10$ ns. Emergence of such loop is due a competition between the hydration effects and the intra-peptide interactions leading to residue-residue contacts along the chain, although there are trapped water molecules. The interplay can be deduced from the non-monotonous behavior of the squared radius of gyration R_g^2 as function of time in Fig. 1(b), obtained from 5 independent runs. Note that for all the cases R_g^2 decays eventually to the equilibrium value.

In order to probe further the structural evolution of the chain along the collapse of (Gly)₂₀, we calculate the static structure factor $S(q)$ at different times. Fig. 1(c) shows $S(q)$ for the times corresponding to the snapshots. At $t = 0$ ns, within the range $q \in [3, 30]$ nm⁻¹, the chain can be described as an extended coil with $S(q) \sim q^{-1/\nu}$ [32], where $\nu = 3/5$ is the critical exponent describing the scaling of $R_g \sim N^\nu$ for a self-avoiding polymer. With time the decay exponent should increase from $-5/3$ and is expected to approach -4 , in order to be consistent with the globule-like behavior of $S(q) \sim q^{-4}$ [32]. Although the slope in our data in Fig. 1(c) gradually increases with time, it does not appear to approach -4 . This again could be due to the still ongoing interplay between the hydration effect and the intra-peptide interactions which hinders the chain to form a compact globule, however, extending the simulations up to 20 ns does not change the overall behavior. Similar observations are made for all systems (Gly)_{*N*} having a chain length of $N < 50$ residue units.

For longer chains, the collapse is more pronounced, and we finally encounter characteristic features reminiscent of the homopolymer collapse. For instance, in Fig. 2(a), we present snapshots of the collapse of (Gly)₂₀₀ at $T_q = 290$ K. The sequence of these snapshots demonstrates a process that starts with local ordering of the residues along the chain. These local structures later merge with each other before finally forming a single globule at $t \approx 20$ ns. The emergence of these local arrangements is similar to the formation of local clusters in the “pearl-necklace” picture of homopolymer collapse [14, 16, 20, 21]. The resemblance becomes even more obvious when looking at the corresponding contact maps in the lower panel. The box-like clustering along the diagonal indicates formation of “pearls” along the chain (see particularly at $t = 2$ and 5 ns) that are reminiscent to the ones observed during the collapse of semiflexible homopolymer in Ref. [27]. However, we do not see the anti-parallel hairpins that were associated with this diamond-shaped internal orders within these boxes.

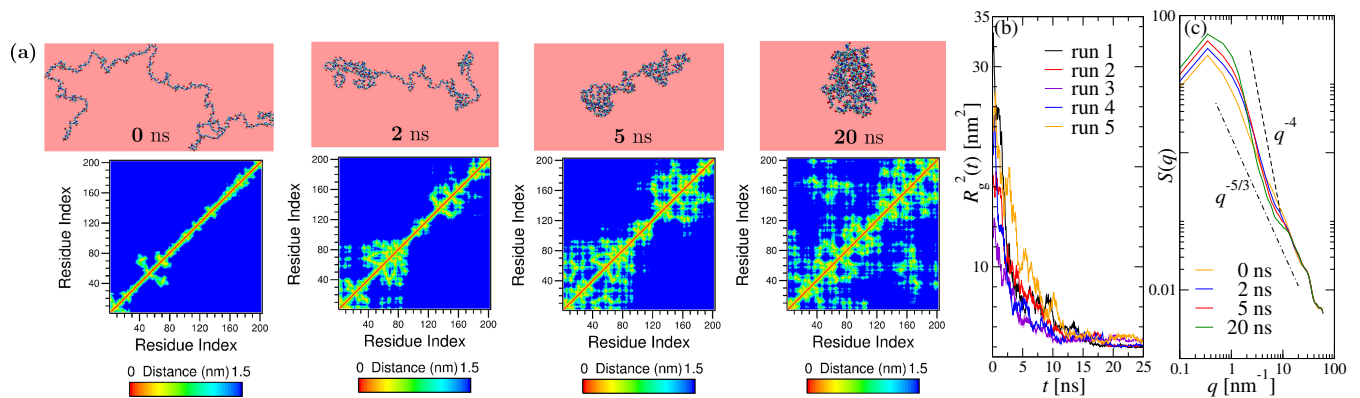


FIG. 2. **Pearl-necklace formation during collapse of longer chains.** (a) Same as in Fig. 1(a) but for $(\text{Gly})_{200}$ and correspondingly at different times, as mentioned. (b) Time dependence of the squared radius of gyration $R_g^2(t)$ from 5 different runs. (c) The structure factors $S(q)$ at times that are presented in (a). There dashed lines have the same meaning as in Fig. 1 (c).

In order to check for the presence of a competition between hydration effects and the intra-peptide interactions we probe again the time dependence of R_g^2 as measured in five independent runs. Data are presented in Fig. 2(b). Unlike for the shorter $(\text{Gly})_{20}$ chain, the radius of gyration is now monotonically decreasing. This can be explained by the assumption that for longer chains the intra-chain interactions overcome the hydration effects. A similar picture emerges from Fig. 2(c). The plots of the structure factor $S(q)$ as function of time demonstrate how the extended coil behavior of $S(q) \sim q^{-5/3}$ at $t = 0$ ns gradually changes to a globule-like behavior of $S(q) \sim q^{-4}$ at $t = 20$ ns.

Next, we analyze the number of intra-molecular, i.e., protein-protein n_{pp} and inter-molecular, i.e., protein-water n_{pw} hydrogen (H)-bonds. These quantities, measured for different N and normalized by the respective values at t_f (the maximum time up to which the simulations are run; for details see the Method section) are plotted as function of time in the main frame of Fig. 3(a) and (b). Data for all N in Fig. 3(a) attain the value ≈ 1 at the same time, demonstrating a reasonable overlap of the normalized data. Similarly happens in (b) the decay of n_{pw} to the saturation value at almost the same time for different N , leading again to nicely overlapping curves. In the inset of Fig. 3(a), the time dependence of n_{pp} for $(\text{Gly})_{20}$ is non-monotonous whereas the n_{pw} data in the inset of Fig. 3(b) exhibit a jump at early time before reaching saturation. This again confirms the hydration effects for smaller chains. The overlap of the hydrogen-bond kinetics for large N indicates that the collapse is not guided by the intra-peptide hydrogen bonds but depends mostly on the intra-peptide van der Waals interactions.

However, the overlap of the hydrogen-bond data does not allow one to calculate the collapse time τ_c from the time evolution of this quantity. More suitable for this purpose is the decay of the average squared radius of gyration

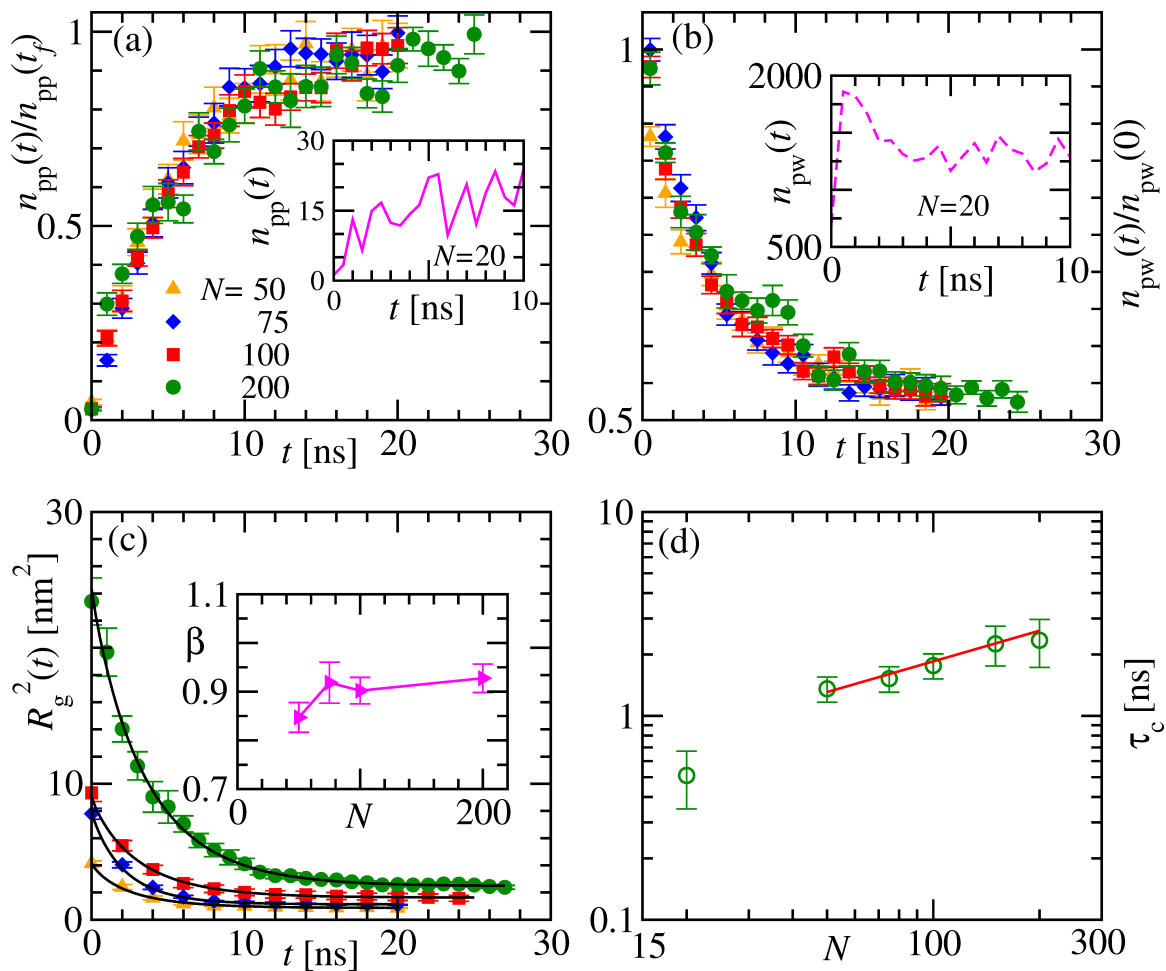


FIG. 3. **Kinetics of H-bonding and scaling of the collapse time.** (a) Time dependence of the number of protein-protein hydrogen bonds $n_{pp}(t)$ during collapse of $(\text{Gly})_N$ for different N . To make the curves fall within the same scale the data is normalized with $n_{pp}(t_f)$; t_f is the maximum run time the simulations are done. The inset shows time dependence of $n_{pp}(t)$ for $(\text{Gly})_{20}$. (b) Same as in (a) but for the number of protein-water hydrogen bonds $n_{pw}(t)$. The inset again is same as the inset of (a) but for $n_{pw}(t)$. (c) Variation of the average squared radius of gyration $R_g^2(t)$ with time for the same systems that are presented in (a) and (b). The solid black lines are respective fits using the form (1) and the corresponding β obtained is shown as a function of N in the inset. (d) Dependence of the collapse times τ_c , extracted from the time decay of R_g^2 on the number of residue N . The solid line represents the behavior $\tau_c \sim N^z$ with $z = 0.5$.

R_g^2 depicted in Fig. 3(c). The non-overlapping data are consistent with the respective solid lines obtained from the previously proposed fit [16, 17]

$$R_g^2(t) = b_0 + b_1 \exp[-(t/\tau_c)^\beta], \quad (1)$$

where b_0 corresponds to the value of $R_g^2(t)$ in the collapsed state, and b_1 and β are associated non-trivial fitting

parameters. The obtained values of β [see the inset of Fig. 3(c)] indicate a very weak dependence on N , similar to the case of the earlier studied collapse of synthetic homopolymers [16]. Although the above fit yields a collapse time τ_c , more accurate estimates can be calculated from the time when $R_g^2(t)$ has decayed to 50% of its total decay, i.e., $\Delta R_g^2 = R_g^2(0) - R_g^2(t_f)$. We plot the measured values of τ_c for different chain length N (including $N = 20$) in Fig. 3(d) to check for a scaling of the form $\tau_c \sim N^z$. Due to the competition between hydration effects and intra-peptide interactions that dominate for smaller N one expects distinct scaling forms for small and large N . Our data indeed hint at the existence of two such scaling regions. Especially interesting is the consistency of our data for large N with the solid line having $z = 0.5$. This exponent suggests that the dynamics is faster than the one observed in MC simulations of non-biological homopolymer [16]. Surprisingly, it is even faster than in the case of homopolymer collapse in presence of hydrodynamics [22, 23]. We conjecture that the more rapid collapse is due to the almost instantaneous presence of intra-chain hydrogen bonds that hasten local ordering. Simulations of longer chains would be desirable to confirm the value of $z = 0.5$ and the super-fast collapse mechanism in hydrogen-bonded polymers, however, such simulations were computationally too costly to be considered in the present study.

In a final step we want to quantify the coarsening kinetics of the “pearl-necklace” observed in Fig. 2(a). A measure of the relevant length scale, i.e., the mean cluster or pearl size $C_s(t)$, can be obtained from a box-plot analysis of the contact maps [27]. Conjecturing that the collapse is driven by the intra-peptide van der Waals attraction of the backbone, we extract $C_s(t)$ from an analysis of the contact probability $P(c_{ij})$ as a function of the contour distance $c_{ij} = |i - j|$ between any two $C\alpha$ -atoms at the i -th and j -th position along the chain [33]. Two $C\alpha$ -atoms are said to have a contact if they are within a cut-off distance r_c . Using $r_c = 2.5$ nm, we show in Fig. 4(a) values of $P(c_{ij})$ calculated at different times during the collapse of $(\text{Gly})_{100}$. These contact probabilities indicate indeed a growing length scale as their decay slows with time. At the beginning, for $t = 0$ ns, the chain is in extended state and $P(c_{ij})$ decays according to a power law $P(c_{ij}) \sim c_{ij}^{-\gamma}$ with an exponent $\gamma = 1.5$, as expected in a good solvent [34]. As time progresses, this power-law behavior appears at larger c_{ij} after crossing over from a plateau-like behavior for small c_{ij} which marks the local ordering along the chain. For any reasonable choice of r_c the form of the curves stays unchanged as demonstrated in Fig. 4(b). Similarly, the form of the curve also does not depend on the chain length N as illustrated in the inset of Fig. 4(b) where we use $r_c = 2.5$ nm and choose the point in time $t = 2$ ns.

The crossover point in the decay $P(c_{ij})$ as a function of c_{ij} is estimated from the discrete local slope as calculated by [33]

$$\gamma_t(c_{ij}) = \frac{\Delta \ln[P(c_{ij})]}{\Delta \ln[c_{ij}]} \quad (2)$$

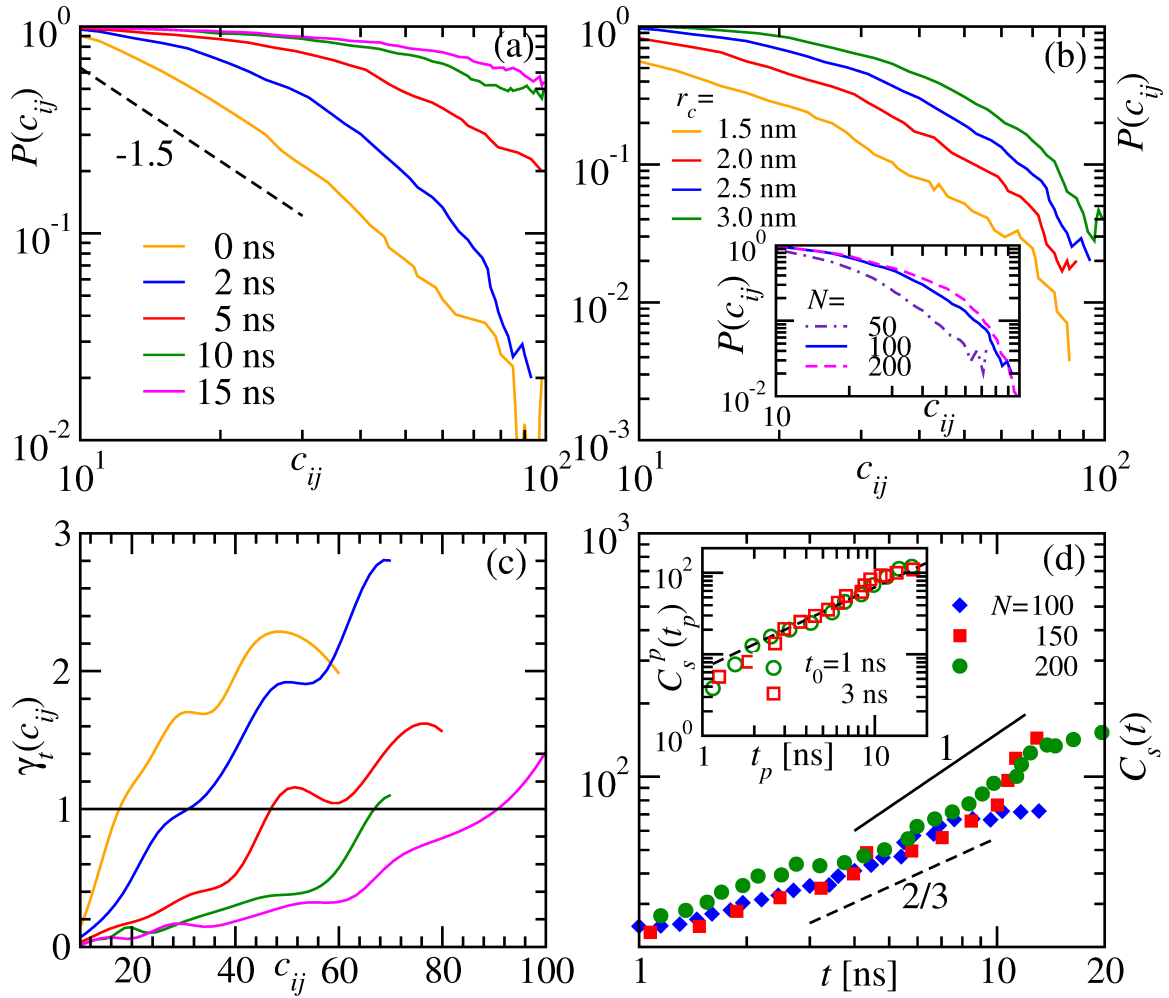


FIG. 4. **Cluster growth during the collapse.** (a) Contact probability $P(c_{ij})$ calculated using the cut-off $r_c = 2.5$ nm, as a function of the distance c_{ij} along the chain, at five different times during collapse of $(\text{Gly})_{100}$. (b) Shows the consistency or the proportionality behavior of estimated contact probability $P(c_{ij})$ at a fixed time $t = 2$ ns using different r_c as indicated. The inset shows $P(c_{ij})$ at $t = 2$ ns using $r_c = 2.5$ nm for different N . (c) The discrete slope γ_t obtained from Eq. (2) as a function of c_{ij} for the times presented in (a). The solid line is for $\gamma_t = 1$. (d) The main frame shows the growth of the mean cluster or pearl size $C_s(t)$ with time for different N . The solid lines represent power-law behavior $C_s(t) \sim t^\alpha$ with $\alpha = 1$ and $2/3$, respectively. The inset shows the plot of $C_s^p(t_p)$ as function of the shifted time $t_p = t - t_0$ for two different choices of t_0 . The solid line there represents a linear behavior.

Plots of $\gamma_t(c_{ij})$ as a function of c_{ij} are shown Fig. 4(c) for the data presented in Fig. 4(a). The crossing of the data with the $\gamma_t = 1$ line happens at larger c_{ij} as t increases, and thus this crossover point gives a measure of $C_s(t)$. The obtained $C_s(t)$ for three different N are shown as a function of t on a double-log scale in the main frame of Fig. 4(d). The flattening of the data at very large t is due to finite-size effects when no more ordering is possible due to formation

of single globule. At large t , before hitting size effects, the growth resembles a power law $C_s(t) = A_N t^\alpha$ where the amplitude A_N depends still on the chain length N as the considered N are not large enough. Hence, $P(c_{ij})$ calculated using the same r_c will overlap with each other, a fact that is demonstrated in the inset of Fig. 4(b). However, since their form stays invariant in the large t regime, they apparently follow the same power law. Our data do not span over decades in time, hence, it is hard to distinguish between $\alpha = 2/3$ and 1 behavior as shown by the dashed and the solid lines, respectively. In such cases it is advantageous to describe the growth instead as $C_s(t) = C(t_0) + A_N(t - t_0)^\alpha$ by considering a crossover time t_0 and cluster size $C(t_0)$. This ansatz, originally developed for ferromagnets [35], was already necessary in our earlier work for describing the collapse of synthetic homopolymers [14, 16, 17]. Using the transformation $C_s^p(t_p) = C_s(t) - C(t_0)$ one finds $C_s^p(t_p) = A_N t_p^\alpha$, with the shifted time $t_p = t - t_0$. For $\alpha = 1$, the above transformation is invariant under any choice of t_0 in the post-crossover regime. This is demonstrated in the inset of Fig. 4(d). The consistency of our data with the solid line representing a linear behavior further consolidates our finding of a linear cluster growth.

In summary, we have investigated the nonequilibrium pathways by which polyglycine collapses in water. For short chains, the pathway has few noticeable features and is driven by the competition between the hydration of the peptide, opposing the collapse, and the intra-peptide attractions, favoring the collapse [7]. For long enough chains the importance of hydration effects decreases, and the kinetics of hydrogen bonds indicates that van der Waals interactions of the backbone dominate and drive the collapse. The nonequilibrium intermediates seen during the collapse exhibit local ordering or clustering that is analogous to the phenomenological “pearl-necklace” picture known to be valid for the earlier studied coarse-grained homopolymer models [20]. Using the contact probability of the C α -atoms in the backbone, we extract a relevant dynamic length scale, i.e., cluster size, that as in simple homopolymer models grows linearly with time [16]. We believe that this linear growth is a result of the Brownian motion of the clusters and subsequent coalescence as in the case of droplet growth in fluids [36].

Especially intriguing is that the scaling of the collapse time with length of the chain indicates a faster dynamics, with a critical exponent $z = 0.5$ instead of $z = 1$, as seen in earlier homopolymer collapse studies [22, 23] that considered simplified models describing non-hydrogen-bonded polymers such as polyethylene and polystyrene [37]. The smaller exponent suggests that the fast folding times of proteins (typically in the $\mu\text{s} - \text{ms}$ range for proteins with $\approx 100 - 200$ residues) may be connected with a mechanism that allows in amino acid based polymers a more rapid collapse than seen in non-biological homopolymers, where collapse times of ≈ 300 ms [38] up to ≈ 350 s [39] for poly(N-isopropylacrylamide) and polystyrene, respectively, have been reported. This would also have implications for

possible folding mechanisms as the fast collapse times in our simulations are connected with a quick appearance of local ordering. In fact, we conjecture that the smaller exponent z is characteristic for collapse transitions where the presence of intra-chain hydrogen bonding in amino acid based polymers immediately seeds (transient) local ordering, a step that in non-hydrogen-bonded polymers only happens as the consequence of diffusive motion. However, in order to test this conjecture, one would need to repeat first our above investigation for the other 19 amino acids. While such study is beyond the scope of our current paper, the presented results demonstrate already that our approach provides a general platform to understand various conformational transitions that occur in biomolecules via local ordering. Another example would be, for instance, the helix-coil transition of polyalanine where the short-time dynamics has already been explored [40, 41], or the study of two-time properties such as aging and dynamical scaling in collapse and folding [15, 17].

METHODS

We construct $(\text{Gly})_N$ molecules with hydrogenated N-terminus ($-\text{NH}_2$) and C-terminus ($-\text{COOH}$). All-atom MD simulations are performed using standard GROMACS 5.0.2 tools while CHARMM22 with CMAP corrections [42, 43] is used for interactions between the atoms. For studying the collapse dynamics, we first prepare an extended chain in gas phase at 1500 K. This follows solvation of this extended chain in a simple cubic box with water (modeled by the TIP3P model [44]). The final MD run is performed at the desired quench temperature $T_q = 290$ K which is lower than 310 K, roughly the collapse transition temperature of $(\text{Gly})_N$ in water. The size of the box and the number of water molecules, of course, are dependent on N and are so chosen that the number density of water molecules is same for all N . For the smallest N , i.e., for $N = 20$ the default box size was 4.2 nm. Subsequently, the box sizes for longer chains were determined using the relation $R_g \sim N^{3/5}$. The size of the boxes should not have much role in collapse provided the two ends of the chain do not interact while using the periodic boundary condition. However, the number density of water molecules is supposed to play a role which we kept the same for all N . For $N = 20$ the total number of water molecules used was ≈ 2000 giving a number density of ≈ 32 per nm^{-3} which was maintained for all N . After the solvation we run our MD simulations using the Verlet-velocity integration scheme with time step $\delta t = 2$ fs, in the NVT ensemble using the Nosé-Hoover thermostat that conserves the linear momentum, and thus is believed to be sufficient for preserving hydrodynamic effects [45]. Here, we use chains of length $N \in [20, 50, 75, 100, 150, 200]$, and all the results presented are averaged over 50 different initial configurations, except for $N = 200$ where this number is 15. The simulations are run up to time t_f which is 10 ns for $N = 20$, 20 ns for $N \in [50, 150]$, and 25 ns for $N = 200$.

For a polymer of length N (number of monomers) the squared radius of gyration is calculated as $R_g^2 = \sum_{ij} (\vec{r}_i - \vec{r}_j)^2 / 2N^2$. For $(\text{Gly})_N$ the chain length was determined from N , the number of residues or repeating units which contain a fixed set of atoms. Thus R_g for $(\text{Gly})_N$ was calculated considering all the atoms present in all the residues. However, the scaling can still be checked in terms N , as is done here. The structure factor for a polymer of length N is calculated using the relation $S(\vec{q}) = (1/N) \sum_{ij} \exp(-i\vec{q} \cdot \vec{r}_{ij})$, where \vec{r}_{ij} is the distance vector between the i -th and j -th monomer along the chain. As explained above in the case for measuring R_g , for $S(q)$ too we use all the atoms in all the residues. We calculate the hydrogen bonds using the standard GROMACS tool `gmx hbond`. It considers all possible donars and acceptors and decides for the existence of a hydrogen bond if the distance between them is less than 0.35 nm and the hydrogen-donar-acceptor angle is less than 30° .

ACKNOWLEDGMENTS

This project was funded by the Deutsche Forschungsgemeinschaft (DFG) under Grant Nos. SFB/TRR 102 (project B04) and JA 483/33-1 and the National Institutes of Health (NIH) under grants GM120578 and GM120634. It was further supported by the Deutsch-Französische Hochschule (DFH-UFA) through the Doctoral College “ \mathbb{L}^4 ” under Grant No. CDFA-02-07 and the Leipzig Graduate School of Natural Sciences “BuildMoNa”. U.H. thanks the Institut für Theoretische Physik and especially the Janke group for kind hospitality during his sabbatical stay at Universität Leipzig.

CONTRIBUTIONS

All authors contributed to develop the project and S.M. performed the simulations. All authors discussed, analyzed the results and wrote the manuscript.

COMPETING FINANCIAL INTERESTS

The authors declare that they have no competing financial interests.

[1] W.H. Stockmayer, “Problems of the statistical thermodynamics of dilute polymer solutions,” *Macromol. Chem. Phys.* **35**, 54 (1960).

- [2] I. Nishio, S.-T. Sun, G. Swislow, and T. Tanaka, "First observation of the coil-globule transition in a single polymer chain," *Nature* **281**, 208 (1979).
- [3] L. Pollack, M.W. Tate, A.C. Finnefrock, C. Kalidas, S. Trotter, N.C. Darnton, L. Lurio, R.H. Austin, C.A. Batt, S.M. Gruner, and S.G.J. Mochrie, "Time resolved collapse of a folding protein observed with small angle x-ray scattering," *Phys. Rev. Lett.* **86**, 4962 (2001).
- [4] M. Sadqi, L.J. Lapidus, and V. Muñoz, "How fast is protein hydrophobic collapse?" *Proc. Natl. Acad. Sci. U.S.A.* **100**, 12117 (2003).
- [5] C.J. Camacho and D. Thirumalai, "Kinetics and thermodynamics of folding in model proteins," *Proc. Natl. Acad. Sci. U.S.A.* **90**, 6369 (1993).
- [6] G. Reddy and D. Thirumalai, "Collapse precedes folding in denaturant-dependent assembly of ubiquitin," *J. Phys. Chem. B* **121**, 995 (2017).
- [7] D. Asthagiri, D. Karandur, D.S. Tomar, and B.M. Pettitt, "Intramolecular interactions overcome hydration to drive the collapse transition of gly15," *J. Phys. Chem. B* **121**, 8078 (2017).
- [8] W. Kauzmann, "Some factors in the interpretation of protein denaturation1," *Adv. Protein Chem.* **14**, 1 (1959).
- [9] K.A. Dill, "Dominant forces in protein folding," *Biochemistry* **29**, 7133 (1990).
- [10] D.W. Bolen and G.D. Rose, "Structure and energetics of the hydrogen-bonded backbone in protein folding," *Ann. Rev. Biochem.* **77**, 339 (2008).
- [11] H.T. Tran, A. Mao, and R.V. Pappu, "Role of backbone-solvent interactions in determining conformational equilibria of intrinsically disordered proteins," *J. Am. Chem. Soc.* **130**, 7380–7392 (2008).
- [12] L.M.F. Holthauzen, J. Rösger, and D.W. Bolen, "Hydrogen bonding progressively strengthens upon transfer of the protein urea-denatured state to water and protecting osmolytes," *Biochemistry* **49**, 1310 (2010).
- [13] D.P. Teufel, C.M. Johnson, J.K. Lum, and H. Neuweiler, "Backbone-driven collapse in unfolded protein chains," *J. Mol. Bio.* **409**, 250 (2011).
- [14] S. Majumder and W. Janke, "Cluster coarsening during polymer collapse: Finite-size scaling analysis," *Europhys. Lett.* **110**, 58001 (2015).
- [15] S. Majumder and W. Janke, "Evidence of aging and dynamic scaling in the collapse of a polymer," *Phys. Rev. E* **93**, 032506 (2016).
- [16] S. Majumder, J. Zierenberg, and W. Janke, "Kinetics of polymer collapse: Effect of temperature on cluster growth and aging," *Soft Matter* **13**, 1276 (2017).
- [17] H. Christiansen, S. Majumder, and W. Janke, "Coarsening and aging of lattice polymers: Influence of bond fluctuations," *J. Chem. Phys.* **147**, 094902 (2017).
- [18] A.J. Bray, "Theory of phase-ordering kinetics," *Adv. Phys.* **51**, 481 (2002).

- [19] P.-G. de Gennes, “Kinetics of collapse for a flexible coil,” *J. Phys. Lett.* **46**, 639 (1985).
- [20] A. Halperin and P.M. Goldbart, “Early stages of homopolymer collapse,” *Phys. Rev. E* **61**, 565 (2000).
- [21] A. Byrne, P. Kiernan, D. Green, and K.A. Dawson, “Kinetics of homopolymer collapse,” *J. Chem. Phys.* **102**, 573 (1995).
- [22] C.F. Abrams, N.K. Lee, and S.P. Obukhov, “Collapse dynamics of a polymer chain: Theory and simulation,” *Europhys. Lett.* **59**, 391 (2002).
- [23] N. Kikuchi, J.F. Ryder, C.M. Pooley, and J.M. Yeomans, “Kinetics of the polymer collapse transition: The role of hydrodynamics,” *Phys. Rev. E* **71**, 061804 (2005).
- [24] G. Reddy and A. Yethiraj, “Implicit and explicit solvent models for the simulation of dilute polymer solutions,” *Macromolecules* **39**, 8536 (2006).
- [25] J. Guo, H. Liang, and Z.-G. Wang, “Coil-to-globule transition by dissipative particle dynamics simulation,” *J. Chem. Phys.* **134**, 244904 (2011).
- [26] A. Montesi, M. Pasquali, and F.C. MacKintosh, “Collapse of a semiflexible polymer in poor solvent,” *Phys. Rev. E* **69**, 021916 (2004).
- [27] A. Lappala and E.M. Terentjev, “Raindrop coalescence of polymer chains during coil-globule transition,” *Macromolecules* **46**, 1239 (2013).
- [28] D.K. Wilkins, S.B. Grimshaw, V. Receveur, C.M. Dobson, J.A. Jones, and L.J. Smith, “Hydrodynamic radii of native and denatured proteins measured by pulse field gradient nmr techniques,” *Biochemistry* **38**, 16424 (1999).
- [29] V.N. Uversky, “Natively unfolded proteins: A point where biology waits for physics,” *Protein Sci.* **11**, 739 (2002).
- [30] I.R. Cooke and D.R.M. Williams, “Collapse dynamics of block copolymers in selective solvents: Micelle formation and the effect of chain sequence,” *Macromolecules* **36**, 2149 (2003).
- [31] T.T. Pham, B. Dünweg, and J.R. Prakash, “Collapse dynamics of copolymers in a poor solvent: influence of hydrodynamic interactions and chain sequence,” *Macromolecules* **43**, 10084. (2010).
- [32] M. Rubenstein and R.H. Colby, *Polymer Physics (Chemistry)* (Oxford University Press, Oxford, 2003).
- [33] V.F. Scolari, G. Mercy, R. Koszul, A. Lesne, and J. Mozziconacci, “Kinetic signature of cooperativity in the irreversible collapse of a polymer,” *Phys. Rev. Lett.* **121**, 057801 (2018).
- [34] P.-G. de Gennes, *Scaling Concepts in Polymer Physics* (AIP, Melville, New York, 1980).
- [35] S. Majumder and S.K. Das, “Domain coarsening in two dimensions: Conserved dynamics and finite-size scaling,” *Phys. Rev. E* **81**, 050102 (2010).
- [36] K. Binder and D. Stauffer, “Theory for the slowing down of the relaxation and spinodal decomposition of binary mixtures,” *Phys. Rev. Lett.* **33**, 1006 (1974).
- [37] K. Kremer and G.S. Grest, “Dynamics of entangled linear polymer melts: A molecular-dynamics simulation,” *J. Chem. Phys.* **92**, 5057 (1990).

- [38] J. Xu, Z. Zhu, S. Luo, C. Wu, and S. Liu, “First observation of two-stage collapsing kinetics of a single synthetic polymer chain,” *Phys. Rev. Lett.* **96**, 027802 (2006).
- [39] B. Chu, Q. Ying, and A.Yu. Grosberg, “Two-stage kinetics of single-chain collapse. Polystyrene in cyclohexane,” *Macromolecules* **28**, 180 (1995).
- [40] E. Arashiro, J.R. Drugowich de Felício, and U.H.E. Hansmann, “Short-time dynamics of the helix-coil transition in polypeptides,” *Phys. Rev. E* **73**, 040902 (2006).
- [41] E. Arashiro, J.R. Drugowich de Felício, and U.H.E. Hansmann, “Short-time dynamics of polypeptides,” *J. Chem. Phys.* **126**, 045107 (2007).
- [42] A.D. MacKerell Jr., D. Bashford, M.L.D.R. Bellott, R.L. Dunbrack Jr., J.D. Evanseck, M.J. Field, S. Fischer, J. Gao, H. Guo, S. Ha, *et al.*, “All-atom empirical potential for molecular modeling and dynamics studies of proteins,” *J. Phys. Chem. B* **102**, 3586 (1998).
- [43] A.D. Mackerell Jr., M. Feig, and C.L. Brooks III, “Extending the treatment of backbone energetics in protein force fields: limitations of gas-phase quantum mechanics in reproducing protein conformational distributions in molecular dynamics simulations,” *J. Comp. Chem.* **25**, 1400 (2004).
- [44] W.L. Jorgensen, J. Chandrasekhar, J.D. Madura, R.W. Impey, and M.L. Klein, “Comparison of simple potential functions for simulating liquid water,” *J. Chem. Phys.* **79**, 926 (1983).
- [45] D. Frenkel and B. Smit, *Understanding Molecular Simulations: From Algorithms to Applications* (Academic Press, San Diego, 2002).